Image Cover Sheet

CLASSIFICATION	SYSTEM NUMBER
UNCLASSIFIED	153693

TITLE

ANALYSIS OF ROTOR FORCES IN A SHIP AIRWAKE

System Number:

Patron Number:

Requester:

Notes:

DSIS Use only:

Deliver to: FF

Report Documentation Page

Form Approved
OMB No. 0704-0188

1. REPORT DATE	2. REPORT TYPE	3. DATES COVERED
OCT 1994		**00-00-1994 to 00-00-1994**

4. TITLE AND SUBTITLE	5a. CONTRACT NUMBER
Analysis of Rotor Forces in a Ship Airwake	5b. GRANT NUMBER
	5c. PROGRAM ELEMENT NUMBER
6. AUTHOR(S)	5d. PROJECT NUMBER
	5e. TASK NUMBER
	5f. WORK UNIT NUMBER
7. PERFORMING ORGANIZATION NAME(S) AND ADDRESS(ES) **Defence R&D Canada - Ottawa,3701 Carling Avenue,Ottawa, Ontario K1A 0Z4,**	8. PERFORMING ORGANIZATION REPORT NUMBER
9. SPONSORING/MONITORING AGENCY NAME(S) AND ADDRESS(ES)	10. SPONSOR/MONITOR'S ACRONYM(S)
	11. SPONSOR/MONITOR'S REPORT NUMBER(S)

12. DISTRIBUTION/AVAILABILITY STATEMENT
Approved for public release; distribution unlimited

13. SUPPLEMENTARY NOTES

14. ABSTRACT

15. SUBJECT TERMS

16. SECURITY CLASSIFICATION OF:			17. LIMITATION OF ABSTRACT	18. NUMBER OF PAGES	19a. NAME OF RESPONSIBLE PERSON
a. REPORT	b. ABSTRACT	c. THIS PAGE			
unclassified	**unclassified**	**unclassified**	**Same as Report (SAR)**	**14**	

ANALYSIS OF ROTOR FORCES IN A SHIP AIRWAKE

G. Syms
S.J. Zan
Applied Aerodynamics Laboratory
NRC Institute for Aerospace Research
Montreal Road, Bldg M-2
Ottawa, Ontario K1A 0R6
CANADA

SUMMARY

This paper examines the helicopter/ship dynamic interface by combining both experimental and numerical analyses. The flow field over the flight deck of a frigate model was mapped experimentally in a wind tunnel using both stationary and flying hot-film sensors. Using the velocity time-histories measured in the wind tunnel, a numerical representation of the airwake which shares the same spectral characteristics was generated. A blade-element model of the main rotor of a helicopter was then "flown" in this numerical airwake to determine the steady and unsteady loads acting on the rotor. The results of a set of test simulations indicate: 1) that an increase in unsteady rotor loads occurs when spatial cross-correlation functions are included in the generation of the numerical flow field; 2) that the fluctuating vertical velocity has a greater effect on the unsteady rotor loads than the fluctuating horizontal velocity; 3) that the spectra of unsteady forces and moments show similar broadband and resonant behaviour at different free-stream velocities.

LIST OF SYMBOLS

(χ, ν, ζ)	non-dimensional coordinate system
D	spectral matrix of white-noise sources
H	frequency response matrix of linear system
h_{ij}	transfer functions of linear system
n_i	white-noise source at location i
R_{ij}	turbulent velocity correlation tensor for velocity components i and j
S	spectral matrix of measured signal
(u, v, w)	velocity field
(x, y, z)	dimensional coordinate system of ship
w_i	unsteady vertical velocity at location i
*	conjugate transpose

1. INTRODUCTION

Helicopter flight onto and from the decks of non-aviation ships such as frigates can be considerably more difficult than the execution of the same manoeuvre on land. The helicopter is immersed in the unsteady airwake in the lee of the ship superstructure. This airwake contains significant gradients in mean wind speed and direction as well as increased turbulence intensities compared to those of the natural wind. The mean flow gradients are associated with shear layers that arise due to flow separations from the superstructure. Considering the fact that a typical frigate superstructure is of the same geometric size as a helicopter rotor diameter, it could be expected that the mean flow gradients and unsteady shear layers both will alter the rotor performance, possibly increasing pilot workload. Furthermore the scale of turbulence shed from a superstructure will vary in size with characteristic dimensions less than or equal to the superstructure. Such eddies can also be expected to affect the rotor loads.

Analysis of the helicopter/ship dynamic interface is further complicated by the coupling of the rotor downwash and the airwake. Although sophisticated flight simulators are being developed for the helicopter/ship interface, complete numerical modelling of the coupled problem as part of a real-time simulation is beyond the realm of current capabilities [1]. At present, simulators permit "flight" of a helicopter through a prescribed turbulent flow field based on the premise that the rotor downwash and airwake are uncoupled. Such models provide estimates of rotor forces, which, when integrated with the helicopter equations of motion, can be used to estimate helicopter response in a given flow field.

In this investigation, such a numerical helicopter model is used to predict the steady and unsteady rotor loads arising from immersion of the rotor in the experimentally-determined wake of a generic frigate. The rotor loads are computed using the rotor module of the GENHEL computer code, which was acquired from the United States Naval Air Warfare Center through The Technical Cooperation Program (TTCP), Technical Panel HTP-6.

The goals of the investigation were: (a) to make detailed flow measurements in a wind tunnel of the airwake in the vicinity of a scale model of a generic frigate (obtaining both single-point and multi-point data); (b) to perform a parametric study to assess the degree of rotor detailing required in the numerical model; (c) to calculate mean and unsteady forces produced by a rotor in a suitably-scaled airwake based on the results of (a). Items (a) and (c) are discussed in this paper.

Paper presented at the AGARD FDP Symposium on "Aerodynamics and Aeroacoustics of Rotorcraft" held in Berlin, Germany from 10-13 October 1994 and published in CP-552.

2. EXPERIMENTAL DETAILS

The wind tunnel measurements were carried out in the IAR 0.9m low-speed wind tunnel. A model of the lowest 50 meters of the atmospheric boundary layer was incorporated using the spire technique [2]. This model includes the correct variation of velocity with height, the correct variation of turbulence intensities with height, and reasonable representations of the length scales of turbulence in the boundary layer. For this experiment, the goal was to attain a wind tunnel flow simulation appropriate to a ship travelling at 10 knots into a headwind of 48 knots at 10 metres above sea level. Comparisons of the measured quantities with values expected in the atmosphere for rough sea conditions [3] are shown in Figures 1a and 1b. The mean profiles are in good agreement, although the turbulence intensities are slightly too large in the wind tunnel. This is not considered a serious problem since the development of the airwake would not be affected by small changes in intensity. In Figure 1, the $z = 0$ plane corresponds to sea level, whereas in all subsequent discussion the $z = 0$ plane corresponds to the flight deck.

A three-view drawing of the ship is presented in Figure 2. The geometric scaling of the wind tunnel model is 1:300. The frigate model has a superstructure loosely based on the Canadian Patrol Frigate. The Reynolds number of the experiment, based on the ship beam of 38.1 mm, is about 15×10^3, in excess of the minimum of 11×10^3 recommended in [4]. The flight deck is clearly evident at the stern, and the bull's-eye thereon is the origin of the coordinate system used throughout the report.

The ship-model airwake was measured using TSI cross hot-film anemometers. A quartic function was used to describe the relationship between the cooling velocity and the probe output voltage.

Characteristics of the airwake were determined in three separate phases. In the first phase, the mean and root-mean-square (rms) values of u, v and w were determined over the region (Fig. 3):

χ = -3/2 , -2/2, -1/2 ... 7/2;
ν = 0, -1/8, -2/8 ... -8/8;
ζ = 4/6, 5/6, 6/6 ... 12/6.

The region was surveyed twice; the second time with the probe axis rolled 90° from its orientation during the first survey, in order to measure the third orthogonal velocity component. Because the model was tested at zero yaw, measurements were made on the port side of the model only. Symmetry relationships were invoked to establish the flow on the starboard side of the ship. These measurements, were made at a sample rate of 100 Hz per channel for 10.24 seconds.

In the second phase, measurements were made with a "flying" cross hot-film probe which can correctly obtain flow velocities in a reversing flow but is less effective elsewhere. The flying probe was used because it was recognized that some of the first-phase measurements would be made in a reversing flow, in which case a stationary probe produces misleading results. Only u-component data were obtained from the flying probe because v and w were too small to be resolved accurately. These flying-probe measurements were made over a region somewhat larger than the size of the separation bubble behind the hangar. In this way, a finite volume existed for which data were acquired with both the stationary and flying probes. By carefully examining both sets of data, it was possible to ascertain the boundaries of reversing flow and thus resolve the flow structure of the entire airwake. The details are described in [5].

In the third phase, measurements of cross-spectra and cross-correlations between various points in the flow were made by the simultaneous acquisition of data from two stationary cross-film probes. Only the streamwise and vertical velocity components were measured in this phase as it was thought that the unsteady rotor forces would be most influenced by these flow components. These data were acquired at a height of 9 meters above the deck, which corresponds to the "high hover" position. The locations of the measurement points in this plane are indicated in Figure 4. Measurements were made using a sample-and-hold A/D converter, so that no appreciable time lags would result in the data collected from different films. Such time lags would make accurate determination of cross-spectra and cross-correlations impossible. Data were collected at a sample rate of 2 kHz per channel for 15.36 seconds with a probe spacing of 15 mm, and for 20.48 seconds with a probe spacing of 30 mm. Because of the difficulty in obtaining flow-correlation characteristics at a point directly downstream of a reference point, the stencil of points used for the measurements was a regular grid rotated 45° with respect to the ship axis system. Again, advantage was taken of the symmetry of the geometry in establishing flow-correlation properties.

The data were reduced to full-scale values for presentation. The physics of bluff-body incompressible flow allows the experimenter to choose any two of the length, velocity and time scalings. The geometric scale was fixed at 1:300, the velocity scaling was chosen to be 1:6 and thus the time scaling defaults to 1:50.

The data presented are time-averaged values of the three velocity components and the turbulence intensities of the three velocity components. The turbulence intensities are defined as the standard deviation of the relevant component divided by the time-averaged value of the streamwise velocity at the same location. The velocity time histories recorded in the wind tunnel contain information on the statistical and probabilistic nature of the airwake. The experimental data indicated that the airwake velocities could be considered to be Gaussian.

3. NUMERICAL MODELLING

A. Numerical Airwake

Having collected the wind tunnel data, the next task is to use that data to create a numerical representation of the measured flow field through which the rotor will be "flown".

To numerically generate the unsteady velocity field, a set of independent white-noise sources $n_i(t)$ are filtered through a constant-parameter linear system $h_{ij}(t)$,

$$w_i(t) = \sum_{j=1}^{N} \int_0^T h_{ij}(\tau)\, n_i(t-\tau)\, d\tau \qquad i = 1..N \qquad (1)$$

where N is the number of points in the flow field and T is the maximum lag interval used in computing the correlations. Note that the unsteadiness of only one velocity component is recreated (either w or u), although the algorithm developed below is directly expandable to include all three components if suitable experimental data exist.

If the spectral functions of the white-noise sources, $n_i(t)$, are described by a constant diagonal matrix D, and a matrix S contains the auto- and cross-spectral density functions of the two-point correlation measurements, then the relation

$$D^{-1}S = H^*H \qquad (2)$$

can be written, where S and D are known and H is as yet unknown. Equation (2) is an underdetermined system for the elements of H. If, however, it is assumed that H is lower triangular, then $D^{-1}S$ can be decomposed and written as a matrix multiplied by its conjugate transpose [6]. Having found H, it can be transformed into the time domain, thus generating the necessary transfer functions for equation (1).

The linear system $h_{ij}(t)$, constructed from the spectral matrix H, will create a numerical velocity field with the same statistical properties as the measured airwake. Although no attempt is made to recreate the probabilistic properties of the experimental data, comparison of the probability density and cumulative distribution functions for the numerical and experimental velocity fields shows similar Gaussian behaviour.

The spectral matrix S contains the auto-spectral density functions for all the measured points along the diagonal. Off the diagonal are the cross-spectral density functions of the various pairs of points. An extremely large amount of data would be required to fill the entire matrix accurately. The experiment established the cross-correlation only between a given point and a collection of its neighbours. The stencil of neighbours was the same for all points in the plane and its application to one of the measurement locations is represented by the shaded circles of Figure 4. The remaining cross-correlations were set equal to zero. In the numerical model, this implies that the flow correlation lengths are less than a rotor radius. Spectra were calculated by first computing the appropriate correlation functions and then transforming them into the frequency domain. It is believed that a reasonable compromise was reached between the accuracy of the spectral matrix S and the amount of time required to gather the experimental data required to generate S.

In the language of statistical theory of turbulence, the above algorithm generates an unsteady flow field by computing an approximation to the three-dimensional second-order correlation tensor R_{ij} [7]. The current method treats only one of the diagonal terms since only one velocity component is computed, but as mentioned previously, all three components can be included and an approximation to the full tensor would result. Unlike other methods of simulating turbulence [8, 9], the current one does not require the assumptions of isotropy, homogeneity or a frozen flow field. The last assumption is unnecessary since the measured time histories provide information on the temporal effects on the correlation tensor. The dependence of the tensor on spatial location and separation (i.e. non-homogeneity and anisotropy respectively) is maintained through the discretization of the plane of high hover and the stencil of the two-point measurements.
In summary, the presented method increases the accuracy of the numerical turbulent flow field by using the experimental data to generate the correlation tensor's spatial and temporal

dependence.

B. Computation of Rotor Forces and Moments

The numerical airwake computed in the previous section is used as input to the rotor simulation. The rotor simulated is that of a UH60A Black Hawk helicopter manufactured by Sikorsky Aircraft. The rotor module has been extracted from the full GENHEL code. This module computes the forces and moments on the main rotor given a prescribed helicopter centre of gravity motion, engine setting, control inputs and wind field. Adjustment of the control settings affecting the trim of the helicopter was limited to modifying only the collective pitch. Its value was adjusted so that the mean rotor thrust was approximately equal to the weight of the helicopter when the rotor was placed in the unsteady airwake at high hover. This set of control settings was used for all the simulations presented in this paper.

The rotor model used is derived from a blade-element analysis [10]. Of particular importance with respect to this simulation are the blade-element velocities from which the aerodynamic and inertial loads of the rotor are computed. The numerical airwake provides an increment to the three orthogonal components of the mean airspeed at the centre of gravity which is taken to be 30.9 m/s (or 101 ft/s) - the velocity the rotor would experience in the earth's boundary layer at a position equivalent to high hover. The mean flow field in the airwake is bi-linearly interpolated in the plane of measurement to the various blade-element locations. In addition, the time-varying velocities at the blade-element locations are computed first by generating them at the experimental measurement points using the convolution integrals of equation (1) and then interpolating them in time and space. The effect of the airwake has thus been included in the calculation of the blade-element velocities generating the rotor forces and moments in the presence of an unsteady airwake.

4. THE AIRWAKE - RESULTS AND DISCUSSION

A. Airwake Mean Velocities

Figure 5 presents the variation in the mean streamwise velocity component for several planes above the flight deck. The data presented have been converted to prototype scale. The boundary between the stationary-probe data and flying-probe data corresponds approximately to the boundary of the region for which reversing flow was detected. Inside the boundary, reversing flow exists and thus only the flying-probe data is valid. The agreement across the boundary is excellent. It is evident that for lateral locations more than one beam away from the ship centreline, the ship has little effect on the flow field for the zero degree yaw case, in agreement with other IAR data [11]. Figure 5 indicates that the time-averaged u-component of the velocity is always in the direction of the free-stream. Measurements were not made close enough to the deck to detect the sign change in the mean value of the u-component.

The stationary probe was also capable of resolving the vertical and lateral velocities in the airwake. These velocity magnitudes were an order of magnitude smaller than those of the streamwise component [5]. Similar results were obtained by the Aeronautical Research Laboratory, Australia, examining full-scale measurements on an FFG-7 Frigate for a wind angle of 0 degrees [12]. For both the lateral and vertical velocity components, the largest magnitudes were found on the boundary between the regions where the stationary- and flying-probe data were valid. Thus the possibility exists that the largest lateral and vertical components of velocity exist within the region of reversing flow and thus were not determined; however, it is unlikely that the magnitudes are significantly greater than those that were measured.

B. Airwake Turbulence Intensities

Measurements of the streamwise turbulence indicated that the region of increased turbulence over that in the natural wind is contained, approximately, directly above the flight deck, extending vertically about one hangar height above the top of the hangar. Upstream of the bull's eye and below the top of the hangar, the mean speeds are approaching zero and the streamwise intensities approach 300% [5].

Measurements of the lateral turbulence indicated that the airwake intensities are comparable in magnitude to the streamwise intensities in regions where the stationary-probe data is valid [5]. This observation, supported by the measurements of [4], makes the airwake distinct from the natural wind, wherein the streamwise intensities are generally double those of the lateral and vertical winds. It was not possible to resolve the lateral or vertical velocity components within the region of reversing flow, so intensities were not determined in this region. However, considering the fact that the streamwise and lateral intensities are of similar magnitude away from reversing flow, it would not be unexpected to find similar lateral turbulence intensity magnitudes in the reversing flow, i.e.

up to several hundred percent based on a local mean velocity.

The variation in vertical turbulence intensities over the flight deck is also presented in Figure 5. The intensities are again normalized on the local mean streamwise velocity. The highest levels of intensity are found closer to the deck. Unfortunately, the highest levels occur in the reversing flow region, where measurements could not be made with confidence. Since the vertical intensities are of the same magnitude as the streamwise and lateral intensities, magnitudes of several hundred percent could again be expected upstream of the bull's eye ($x = 0$) for heights below the top of the hangar.

Spectra of the measured and computed vertical velocities determined at high hover directly above the centre of the flight deck are presented in Figure 6. The spectra are presented at prototype scale. At the higher frequencies, the spectra have a slope of -5/3, consistent with all turbulence spectra in the inertial subrange.

5. ROTOR SIMULATION - RESULTS AND DISCUSSIONS

A. Numerical Airwake

The first step in the simulation of the rotor in the airwake was the generation of a numerical representation of the experimentally measured flow field. This involved creating and decomposing the spectral matrix S.

The matrix S consists of the auto-spectral density functions along the diagonal and the measured cross-spectral density functions off the diagonal. When the experimental spectra were combined in S, scatter in the magnitudes of the spectral estimates at low frequencies formed a matrix which was not always positive-definite and thus could not always be decomposed. In each spectra, the low frequencies are the least accurate because of the limited amount of averaging done at the long lag intervals when computing the autocorrelation. A filter thus had to be applied at the low frequencies to ensure positive-definiteness. The effect of this filter on the velocity spectra can be seen in Figure 6. The agreement between the spectra is quite good throughout the frequency range of interest with a deterioration due to the filter evident at the low frequencies. Longer experimental time histories and/or a more accurate method of computing the elements of the matrix should eliminate the need to use a filter.

B. Rotor Forces and Moments

Having obtained a numerical representation of the airwake of a frigate, the numerical helicopter rotor can be "flown" through it. The simulations produce time histories of the unsteady rotor forces and moments which can then be analyzed in the time or frequency domain.

Using the stationary hot-film measurements, steady rotor loads can be computed over a larger domain than simply a plane at high hover. To this end, the rotor was placed in various horizontal planes (with the rotor hub remaining over the origin on the flight deck) to determine the effect of elevation on the mean rotor forces and moments. Figure 7 shows this effect on the Z-force (the vertical force in body axes) and the rolling moment. The solid line shows the response of the rotor to the steady airwake while the dashed line shows the response without the airwake but still including the vertical variation of free-stream velocity in the atmospheric boundary layer. (It must be remembered that the control settings were not modified between simulations.) It can be seen that as the rotor rises out of the airwake, its response approaches that in the free-stream. This trend is relatively smooth due to the fact that these horizontal planes lie above the fluctuating shear layer separating from the hangar deck.

The numerical representation of the airwake includes the spatial variation of three components of the mean flow field in the plane of high hover as well as the temporal variation of one velocity component. Four test cases were run which systematically varied specific flow-field characteristics to examine their effect on the rotor. Three test cases were run with the w velocity component being computed as unsteady since it was believed that this component would have the greatest influence on the rotor [13]. The fourth test case was run with an unsteady u-component instead to examine that assumption.

Of the three test cases run with a fluctuating w-component, one was run with the full spectral matrix S decomposed into its associated frequency response functions. The next case had all the off-diagonal terms in S set to zero to isolate the rotor's response to the auto-spectra. In the final w case, the measured velocity field was scaled by a factor of 2/3 to decrease the free-stream velocity to 20.6 m/s while maintaining the same turbulence intensities and cross-spectral information and using the full matrix.

The results from these four simulations can be found in Table 1 and Figure 8. Table 1 contains the means and standard deviations of all the

	W Unsteady (Full Matrix)		W Unsteady (Diagonal Matrix)		U Unsteady		W Unsteady (20.6 m/s)	
Force (N)	Mean	Std Dev	Mean	Std Dev	Mean	Std Dev	Mean	Std Dev
X	2082	211	2075	154	2076	80	2771	154
Y	-1477	137	-1479	116	-1470	39	-1179	88
Z	-59820	2710	-59744	1863	-59594	646	-54625	1748
Moment (N.m)								
Roll	-6880	1058	-6905	873	-6891	216	-5348	764
Pitch	22951	1515	22960	1149	22841	671	17095	965
Yaw	24557	574	24644	418	25200	193	25867	314

Table 1: Mean and Standard Deviation of Rotor Forces and Moments for Various Test Cases

rotor forces and moments for each case. Again, it must be noted that the collective pitch was the only control input set before all the test cases were run. Notably then, the cyclic pitch was not altered from a nominal trim setting in free-stream conditions. These results show that the omission of the off-diagonal terms reduces in magnitude the unsteady response of the rotor while maintaining the mean forces and moments. A reduction of the standard deviations but not the means also occurs when the u-component is made to fluctuate instead of the w-component. This supports the belief previously stated that the w-component is more important in these rotor simulations. Finally, the effect of decreasing the free-stream velocity simply decreases the mean and standard deviation of the forces and moments.

The unsteady response of the rotor for the four test cases can be examined in the frequency domain. Figure 8 contains the auto-spectral density functions of the Z-force and rolling moment. Information on the other forces and moments can be found in [5]. The rotor responds to the turbulent velocity field in a resonant manner at four different frequencies: 5.2, 17.3, 34.5 and 48.6 Hz. The fact that these frequencies are unchanged when the free-stream velocity is altered indicates that these are structural modes.

6. CONCLUSIONS

This paper has described a combined experimental and numerical approach to determining the steady and unsteady loads produced by a rotor in a ship airwake. The airwake, which was numerically generated based on experimental data, was input into a numerical model of a flying rotor. The mutual interaction between the spinning rotor and the flow field was not modelled. The following conclusions are drawn from this investigation.

1) Turbulence intensities of several hundred percent are present in the reversing flow region behind the hangar and above the flight deck. The intensities are roughly equivalent for all three velocity components.

2) The incorporation of airwake cross-spectral information into the turbulence modelling leads to increased rotor responses over those determined in the absence of cross-spectral information.

3) The fluctuating vertical component of velocity has a greater effect on the unsteady rotor loads than does the fluctuating streamwise component of velocity.

4) If the free-stream wind speed is reduced, the mean and unsteady rotor loads are reduced in magnitude, although the shape of the spectra remain essentially unchanged.

7. REFERENCES

[1] Clement, W.F., Gorder, P.J. and Jewell, W.F. "Development of a Real-Time Simulation of a Ship-Correlated Airwake Model Interfaced with a Rotorcraft Dynamic Model", AIAA/AHS Flight Simulation Technologies Conference, August 1992. AIAA-92-4149-CP.

[2] Irwin, H.P.A.H. "Design and Use of Spires for Natural Wind Simulation" NRC-NAE-LTR-LA-233, 1979.

[3] Cook, N.J. "The Designer's Guide to Wind Loading of Building Structures - Part 1", Butterworths, London, 1985.

[4] Healey, J.V. "Establishing a Database for Flight in the Wakes of Structures", Journal of Aircraft, vol. 29, no. 4, pp. 559-564, Jul-Aug 1992.

[5] Zan, S.J. and Syms, G. "Numerical Prediction of Rotor Forces in an Experimentally-Determined Ship Airwake" NRC-IAR-LTR-AA-15, To be published.

[6] Dodds, C.J. and Robson, J.D., "Partial Coherence in Multivariate Random Processes", Journal of Sound and Vibration, 42(2) 1975.

[7] Hinze, J.O. "Turbulence", McGraw Hill, New York, Second Edition, 1975.

[8] Etkin, B. "Dynamics of Atmospheric Flight", John Wiley & Sons, Toronto, 1972.

[9] Robinson, P.A. and Reid, L.D. "Modelling of Turbulence and Downbursts for Flight Simulators", Journal of Aircraft, Volume 27, Number 8, August 1990.

[10] Howlett, J.J., "UH-60A BLACK HAWK Engineering Simulation Program: Volume 1 Mathematical Model" NASA Contractor Report 166309, 1981.

[11] Zan, S.J. and Garry, E.A. "Wind Tunnel Measurements of the Airwake Behind a Model of a Generic Frigate", NRC-IAR-LTR-AA-13, June 1994.

[12] Gilbert, N. Aeronautical and Maritime Research Laboratories, Melbourne, Personal Communication, 1993.

[13] Funk Jr, J.D. Naval Air Warfare Center, Personal Communication, 1993.

8. ACKNOWLEDGEMENTS

This work was funded in part by the Institute for Aerospace Research of the National Research Council of Canada (IAR/NRC) and in part by the Department of National Defence (DND FE 220792 NRC 05). The authors would like to acknowledge the efforts of Ms. Hui Cai in designing the flying-probe mechanism and of Ms. Stephanie Lavigne in producing the coloured representations of the flow field.

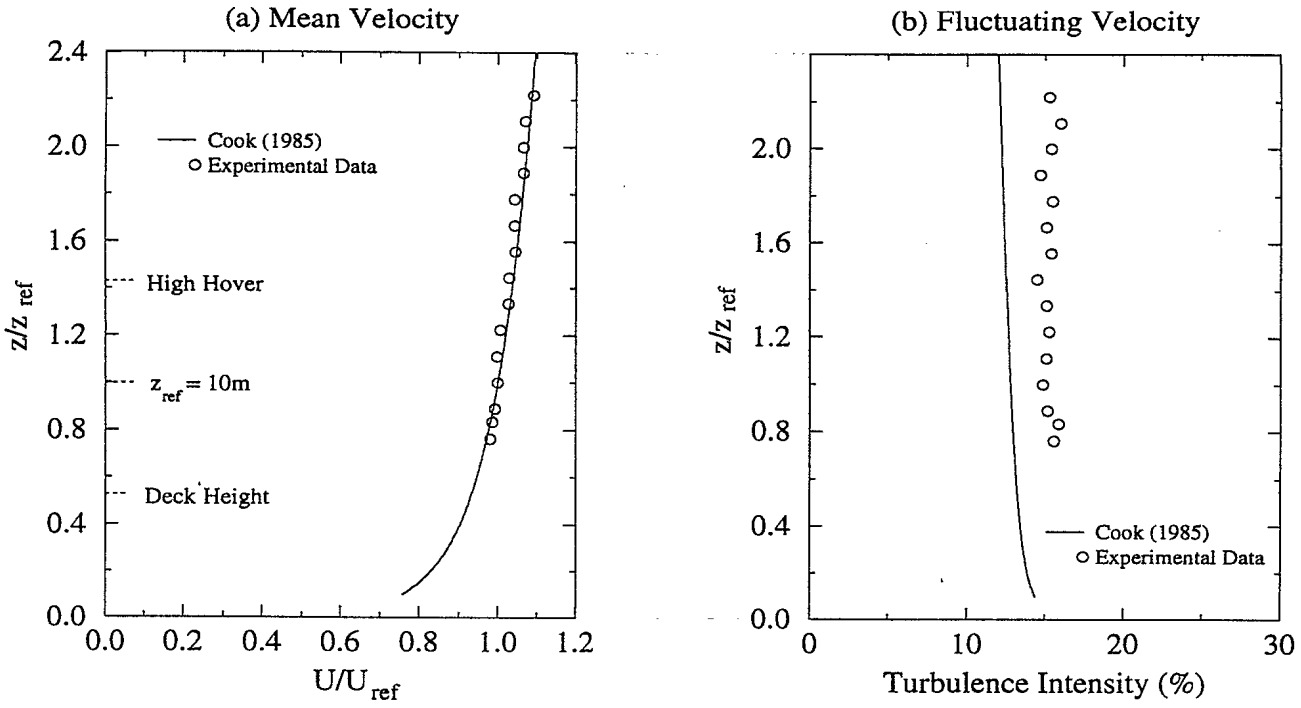

Figure 1: Characteristics of Wind Simulation

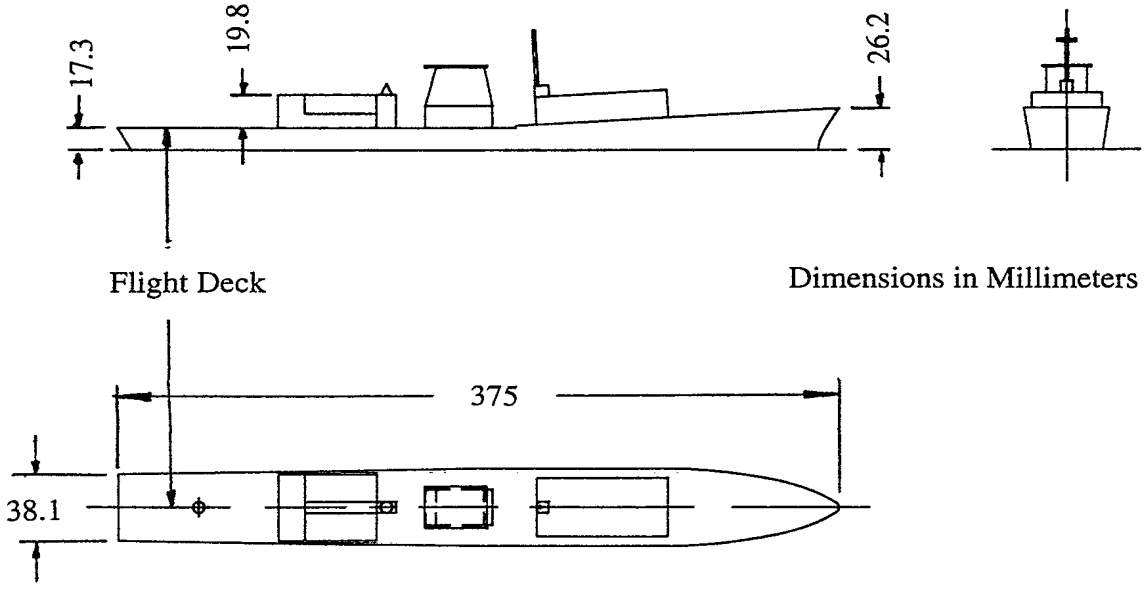

Figure 2: Generic Frigate Model

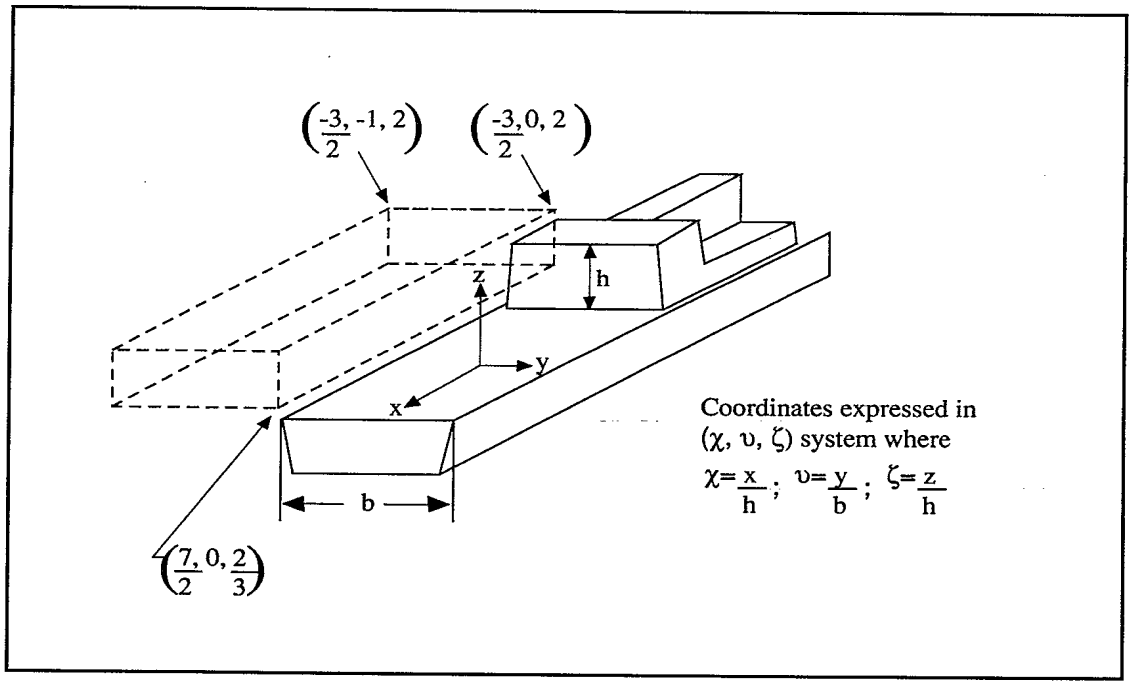

Figure 3: Measurement Volume for Data Acquired with the Fixed Probe

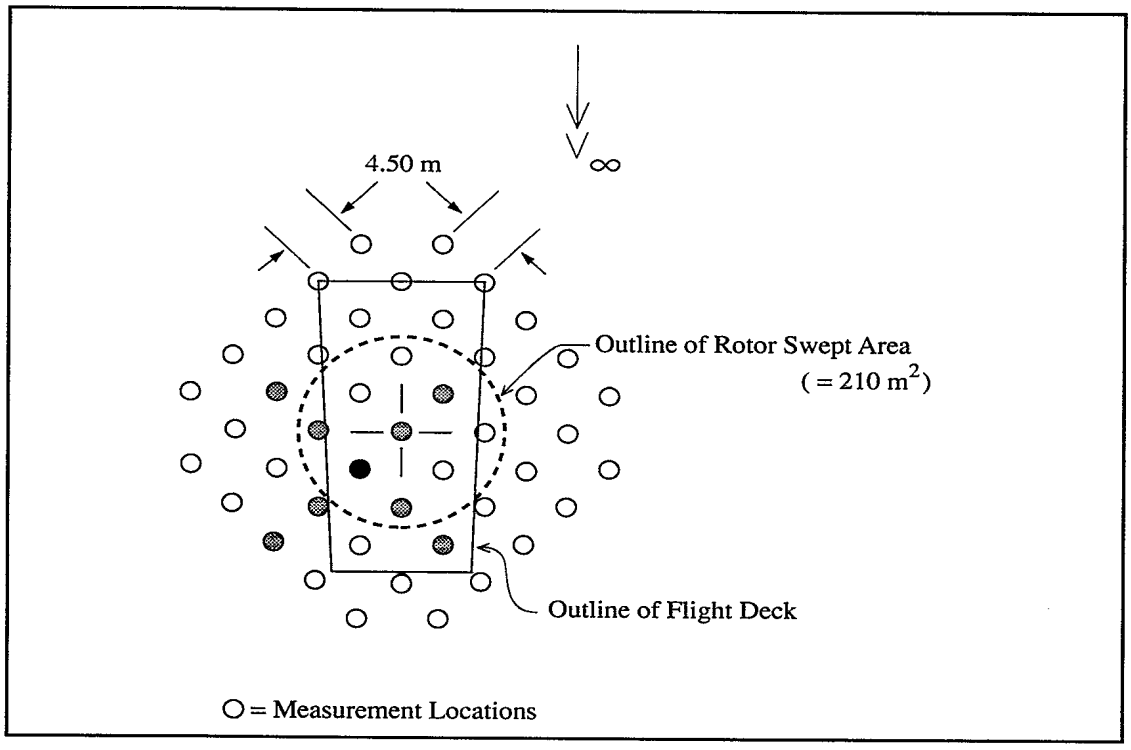

Figure 4: Measurement Locations for Two-Point Correlation Evaluations at High Hover

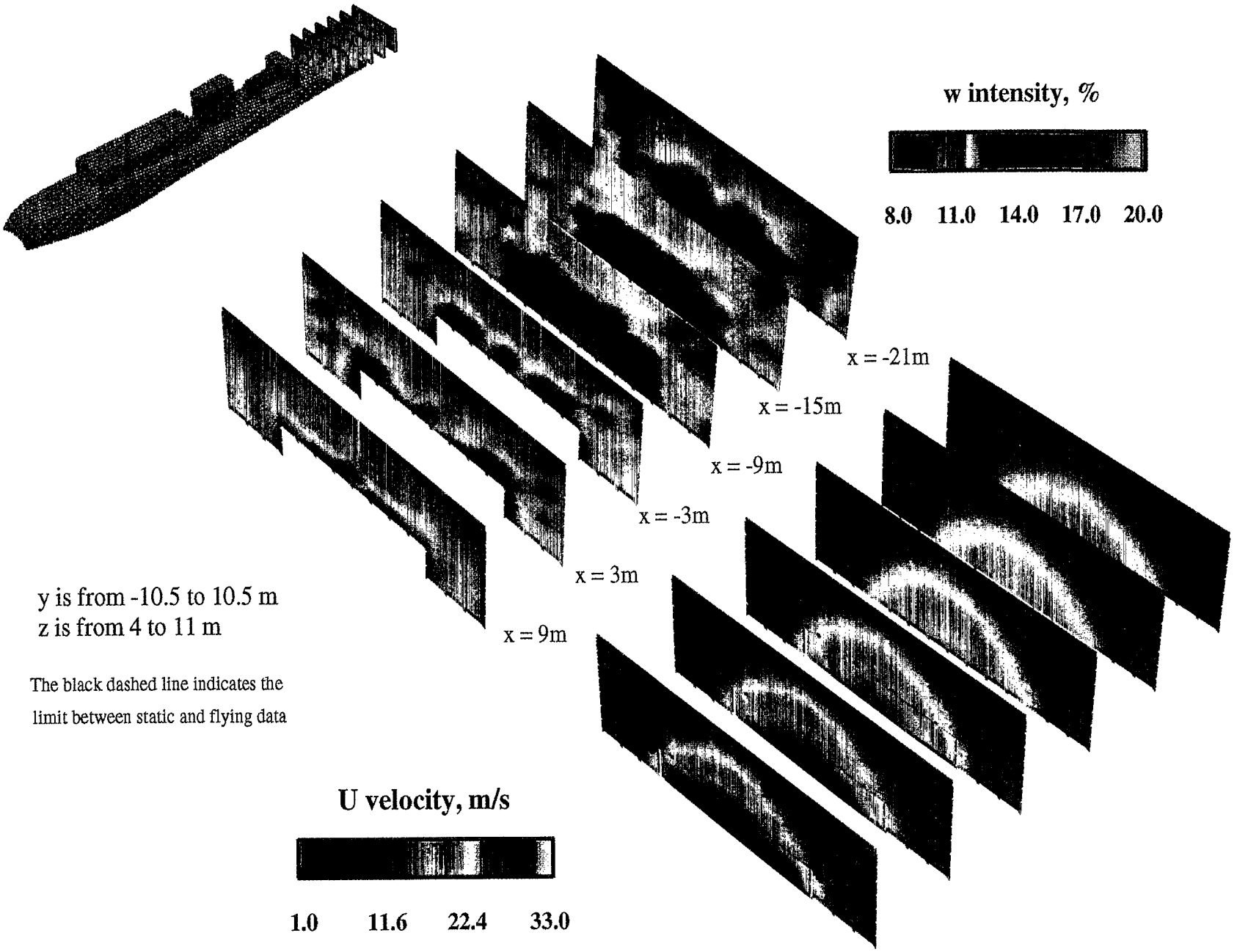

Figure 5. Effect of Streamwise Location on Variation of U Velocity and w Intensity in YZ Planes

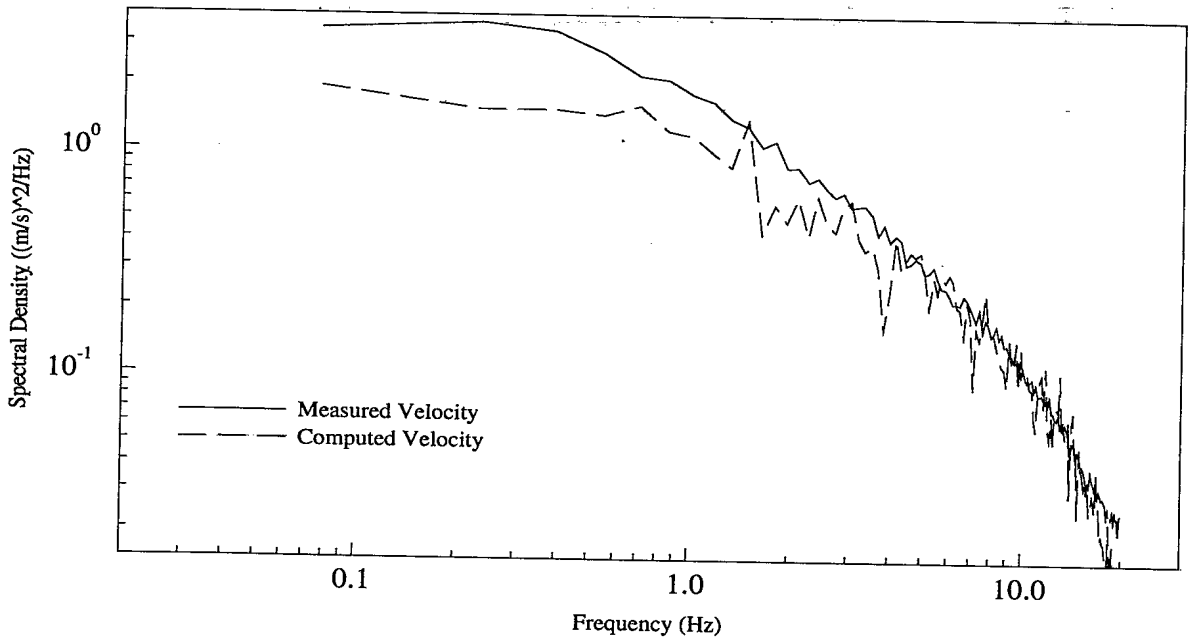

Figure 6: Autospectral Density Function of Vertical Velocity at Centre of Rotor Plane

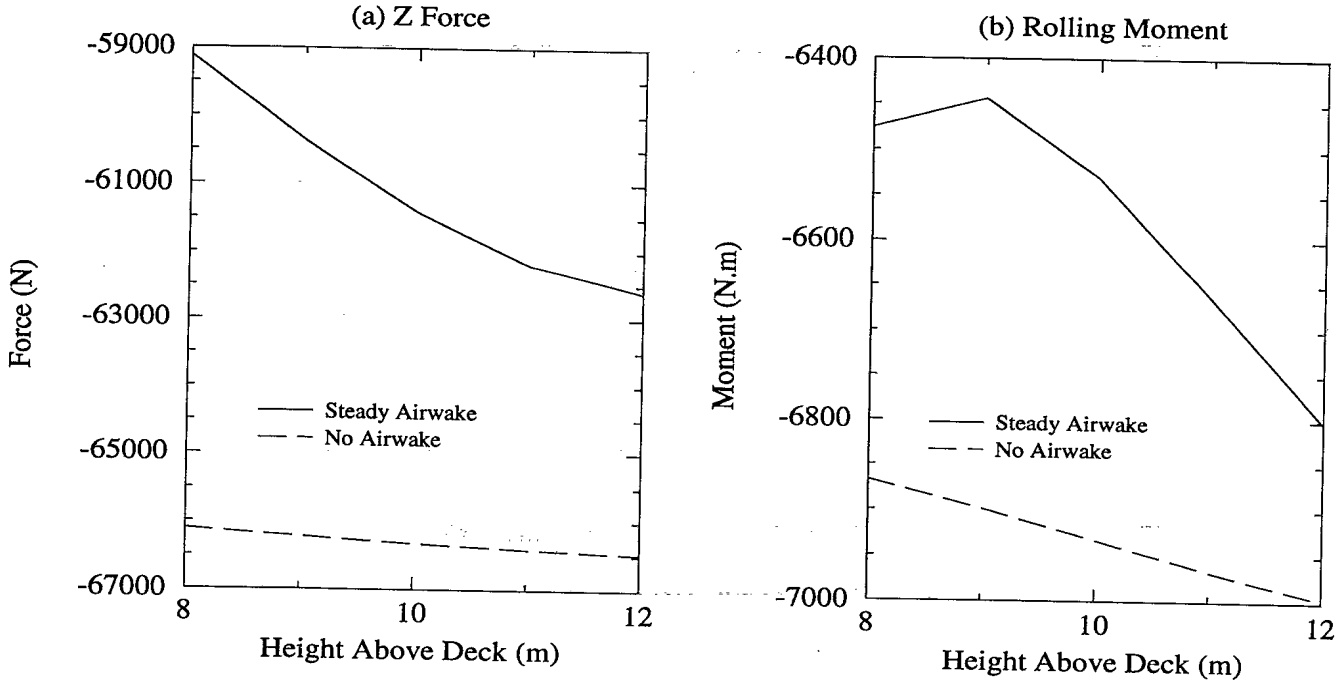

Figure 7: Variation of Rotor Loads with Height Above Deck

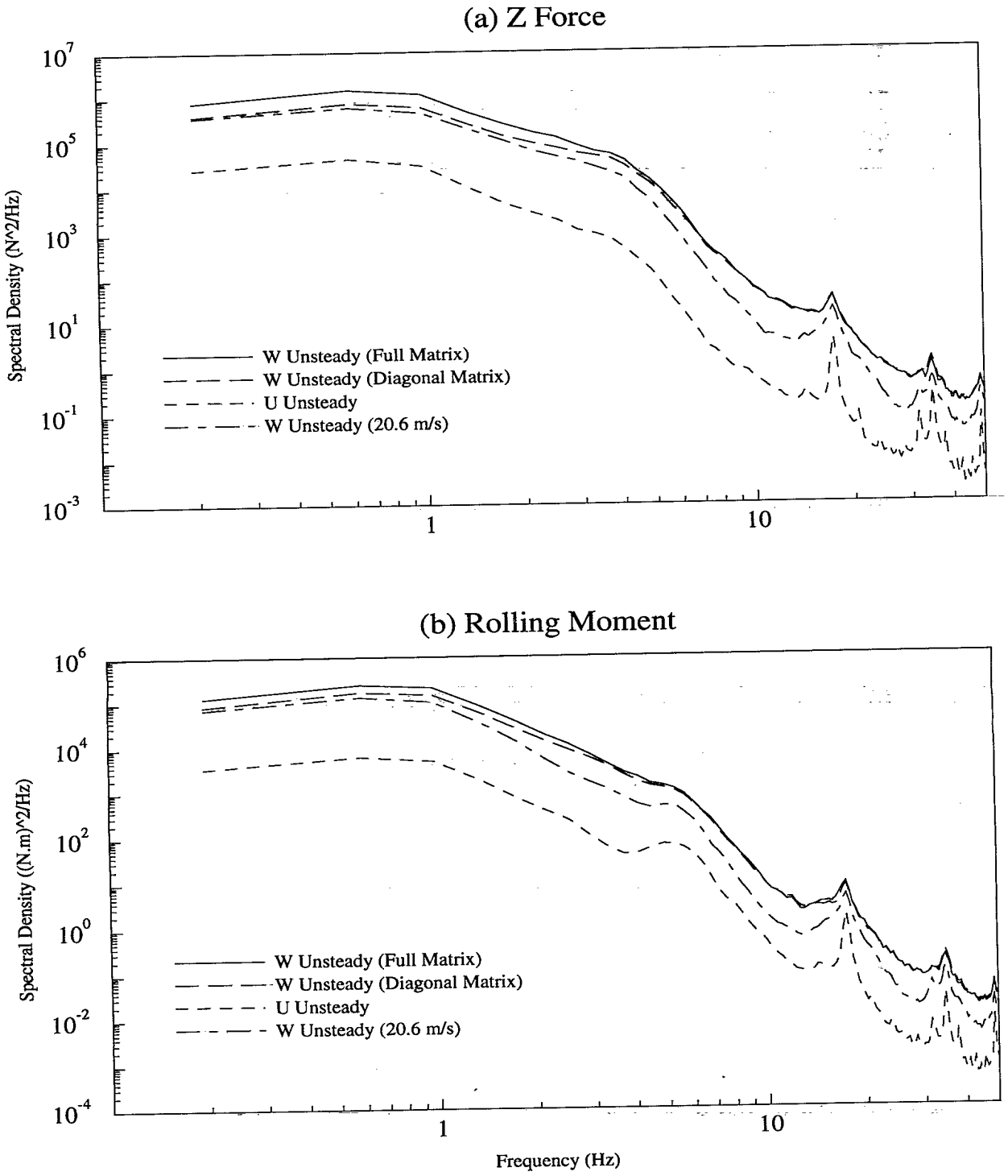

Figure 8: Autospectral Density Function of Rotor Loads
for various Test Conditions